THE JOURNAL OF PHYSICAL CHEMISTRY B

ARTICLE

pubs.acs.org/JPCB

Excitation Energy Transfer in a Non-Markovian Dynamical Disordered Environment: Localization, Narrowing, and Transfer Efficiency

Xin Chen and Robert J. Silbey*

Department of Chemistry and Center for Excitonics, Massachusetts Institute of Technology, Cambridge, Massachusetts 02139, United States

ABSTRACT: The non-Markovian effect of a fluctuating environment plays an important role in electronic excitation transfer in organic disordered media, such as light-harvesting systems and conjugated polymers. Stochastic Liouville equations (SLE) are used to study the interaction between excitons and the environment. We model the non-Markovian environment phenomenologically with a dichotomic process. An exact approach to solve the SLE based on Shapiro and Loginov's differentiation formulas allows us to rigorously study the effect of the non-Markovian environment on excitation energy transfer, such as coherence conservation and its implication for transfer efficiency. This simple SLE model goes beyond the perturbative second-order master equation valid for both the weak coupling and short time correlation conditions. In addition, we discuss why our non-Markovian model is a good approximation to the SLE model driven by the stationary Gauss−Markov process (Ornstein−Uhlenbeck process) over a broad range of fluctuation strengths and correlation times. Numerical results based on our SLE model for dimeric aggregates and the Fenna−Matthews−Olson (FMO) complex reveal the important interplay of intermolecular coupling, correlation time, and fluctuation strength, and their effects on the exciton relaxation process due to the environmental phonon. The results also uncover the connection between localization and motional narrowing, and the efficiency of electronic excitation transfer, demonstrating that the non-Markovian environment is critical for chromophore aggregates to achieve an optimal transfer rate in a noisy environment and to contribute to the robustness of the FMO excitation energy transfer network.

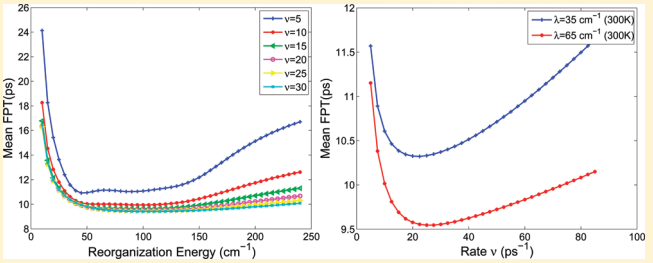

1. INTRODUCTION

The dynamics of excitons in molecular aggregates, such as conjugated polymers and biological light harvesting systems, are strongly affected by the fluctuating environment. Recent experimental studies[1,2] discovered long-lasting coherent motion of populations in these systems. Many interesting questions arise from the new experimental work. Does the long-lasting coherent motion enhance the efficiency of excitation energy transfer? What is the non-Markovian effect in the transfer process? What is the connection between narrowing and localization, and transfer efficiency?

To answer these questions, we need to understand the surrounding protein environment. A first step is to study the effect of the phonon bandwidth of the protein environment. Second, we can look at the effect of the phonon band shape, such as skewness or kurtosis, and the correlation between different local phonons due to their confined protein environment.[3] The phonon bandwidth is intricately connected to the correlation time of the Gaussian colored noise. Having a model to describe colored noise for the whole spectrum of the fluctuation strength and correlation time, particularly for intermediate damping and long correlation time, will help us begin to understand the effect of the environment and theoretically address these questions. In the future, we will study the effect of other phonon band characteristics.

The Redfield equation and its non-Markovian version (both are perturbative second-order equations) have been extensively used to study different limiting cases. This second-order equation has either the partial-ordering prescription (POP) or the chronological-ordering prescription (COP) based on the cumulant expansion or projection operator technique.[4,5] It works well to model multichromophoric systems with weak damping and short correlation time. For strong damping, Förster resonance energy transfer provides a good model. However, perturbative methods are often not sufficient to model non-Markovian dynamics with a long time correlation and intermediate/strong fluctuation damping.

A SLE that includes the fluctuations phenomenologically as a multiplicative stochastic process has a simple form and has been used to study line shapes and transport for excitons.[6−14] The SLE is a set of differential equations whose coefficients are time-dependent random processes. Such problems are often seen in physics and engineering.[15] The theory of multiplicative stochastic processes has a long history in physics, but the equations occurring can rarely be solved because the average of a product of stochastic quantities does not factorize into the product of the averages (although it has been argued by van Kampen[16] that

Special Issue: Shaul Mukamel Festschrift

Received: November 19, 2010
Revised: January 28, 2011
Published: March 08, 2011

good approximations can be derived by assuming such factorizations). This approach, which leads to Bourret's integral equation,[17] can be justified if the driving stochastic process has a short correlation time. The SLE extends the Redfield equation for exciton transport, which is limited to fast fluctuations (short correlation time). It further extends the cumulant expansion method (CME) used for linear coupling of site energies to a heat bath, in particular the perturbative second-order equation in POP or COP prescription. At high temperature, both the CME and Redfield approaches are obtained as limiting cases of the SLE. Naturally, it is very difficult to obtain an exact solution to the SLE with arbitrary spectral characteristics of fluctuations. In addition, the SLE has several limitations: it neglects the system-bath entanglement and assumes an infinite bath temperature. However, these limitations can potentially be partially corrected.[18]

Two types of stochastic models (or processes)[19] are commonly used in the SLE. One is the discrete state jump process, e.g., a dichotomic process, and the other is the continuous state stochastic process, e.g., a Gauss−Markov process. To the authors' knowledge, there are two SLEs that can be solved exactly. One is the Haken−Strobl−Reineker (HSR) model, which considers the extremely broad phonon band compared to the exciton band, taking the phonon fluctuation as a δ-correlated in time Gauss−Markov process. In the limit of such a short correlation time, factorization can be justified. This model has been successfully applied to triplet exciton transport in organic crystals.[6,7] The other model is non-Markovian and includes the phonon fluctuation as a dichotomic process with exponential memory. As a simple model, the dichotomic process has been used to study the non-Markovian effect, from stochastic resonance[20] to line shape narrowing.[21,22] For a dichotomic process, the multitime correlation function can be factorized due to the Bourret−Frisch−Pouquet theorem.[23] We will come back to this in section 3.

In the 1970s, Shapiro and Loginov provided a differentiation formula and analysis[19] to solve the SLE. For any random process in the SLE governed by the Fokker−Planck equation, the equivalent Shapiro and Loginov differentiation formula for moments, defined in section 2, can be found. This differentiation formula is a simple but very powerful mathematical tool to study the SLE and other interesting chemical dynamics questions with noise involved. There are several processes that have the explicit equations of motion for moments, such as the dichotomic process, the Gauss−Markov process, and the Kubo−Anderson process. The dichotomic process and the Gauss−Markov process have the same differential equation for the first-order moment. For the dichotomic process, the Bourret approximation becomes an equality; for the Gauss−Markov process, the Bourret equality becomes an approximation.[24] Thus, the dichotomic process can be considered as a reasonable approximation for the general Gauss−Markov process, or as the consistent first-order truncation of Shapiro and Loginov's differentiation formula for the Gauss−Markov process.[19] As suggested initially by Kubo[25] and later by Tanimura[18] and also Shapiro and Loginov,[19,26] certain truncation schemes for higher order moments can be obtained for the Gauss−Markov process. The numerical sampling method for a stationary Gauss−Markov process (Ornstein−Uhlenbeck process) is now a routine numerical recipe.[27] It can be used to solve the SLE driven by the Gauss−Markov process or even a general fractional Gaussian process to model the structure of random media. In this paper, we will use the exact solutions for the dichotomic process to study non-Markovian effects, localization, and motional narrowing and their connections to the efficiency of excitation energy transfer in the FMO complex.

As for the SLE model that we use to study the influence of colored noise, the two concepts of Markovian approximation and Markovian process (Markovian property) are often confused. A dynamical equation with no memory kernel is often called Markovian; however, the Markov process will, in general, yield a dynamical equation with a memory kernel. Only when this kernel is a delta function in time will there be no memory. A short discussion can be found in Appendix B.

In section 2, we discuss the SLE model driven by the dichotomic process and how to obtain the corresponding equations of motion of moments generated by the Shapiro and Loginov differentiation formulas. In section 3, we discuss the Bourret equality used in section 2 and its relation to the Gaussian process. In section 4, we discuss excitation energy transfer in symmetric dimers and how non-Markovian disorder affects the dynamics of populations and coherences. In section 5, we discuss the non-Markovian effect on the efficiency of excitation transfer in the FMO complex.

2. NON-MARKOVIAN SLE MODEL

The SLE driven by colored noise provides a consistent accounting for fluctuations of arbitrary time scale. The general Hamiltonian for the SLE is

$$H(t) = H_0 + \sigma(t) \tag{1}$$

where H_0 is the deterministic part and $\sigma(t)$ is the nondeterministic part whose matrix elements are independent random variables or stochastic processes with either discrete or continuous states. The stochastic Hamiltonian is defined as

$$\frac{\mathrm{d}}{\mathrm{d}t}\rho(t) = -\mathbb{L}(t)\rho(t) \tag{2}$$

where $\mathbb{L} = i\,[H(t),\cdot\,]$ or in terms of the density matrix elements

$$\frac{\mathrm{d}}{\mathrm{d}t}\rho_{ij}(t) = -\sum_{n,m}\mathbb{L}_{ij;nm}(t)\rho_{nm}(t) \tag{3}$$

where we have $N \times N$ linear differential equations and $\mathbb{L}_{ij;nm}(t) = i\Sigma_k[H_{ik}(t)\delta_{kn}\delta_{mj} - H_{kj}(t)\delta_{in}\delta_{mk}]$. The reduced density matrix is the average value of the density matrix, $\langle\rho_{kl}(t)\rangle$, according to the probability measure of the stochastic process, $\sigma(t)$. In the path integral formalism, the average can be written as

$$\langle\rho(t)\rangle = \langle\exp[-\mathbb{L}_0 t - \int_0^t \mathbb{L}_\sigma(s)\,\mathrm{d}s]\rangle\rho(0)$$

Since the above expression has two noncommutative operators $\mathbb{L}_0$ and $\mathbb{L}_\sigma(s)$, a time-ordered infinite expansion can be generated with the help of the cumulant expansion or projection operator technique[5] to represent the evolution operator, $\langle\exp[-\mathbb{L}_0 t - \int_0^t\mathbb{L}_\sigma(s)\,\mathrm{d}s]\rangle$, exactly. Truncation of the infinite expansion is necessary, and the weak-coupling limit is needed to justify the truncation. The infinite cumulant expansion is unavoidable even for the dichotomic process whose multitime correlation functions can be factorized.

Defining $\langle\rho_{kl}(t)\rangle$ as the zeroth-order moment, and the higher order moments such as $\langle\sigma_{ij}(t)\rho_{kl}(t)\rangle$ and $\langle\sigma_{ij}(t)\sigma_{nm}(t)\rho_{kl}(t)\rangle$, where $\sigma_{ij}(t)$ is the matrix element of $\sigma(t)$, etc., we can generate

the equations of motion of moments with the Shapiro and Loginov differentiation formula.[26] The advantage of this method is that we do not need to consider the time ordering due to the noncommutative operators $\mathbb{L}_0(t)$ and $\mathbb{L}_\sigma(t)$, since the time ordering is implicitly embedded in the formula. We map the dynamics of the reduced density matrix elements, $\langle\rho_{kl}(t)\rangle$, to a set of coupled linear equations. We will discuss how to construct the equations of motion of moments for symmetric dimers as an illuminating example in this section. The generalization for multichromophoric systems will be shown in Appendix A

Without loss of generality, we can define the Hamiltonian for a symmetric dimer as

$$H = \sum_{n=1}^{2} \sigma_n(t)|n\rangle\langle n| + J(|1\rangle\langle 2| + |2\rangle\langle 1|) \tag{4}$$

where we assume the two site energies, $\varepsilon_1 = \varepsilon_2 = 0$, and the two diagonal fluctuations, $\sigma_1(t)$ and $\sigma_2(t)$, are independent dichotomic processes. The compact form of the SLE can be defined as

$$\frac{\mathrm{d}}{\mathrm{d}t}\hat{\rho} = -\mathbb{L}\hat{\rho}$$

where $\hat{\rho} = (\rho_{11}, \rho_{22}, \rho_{12}, \rho_{21})$, and

$$\mathbb{L} = \mathbb{L}_0 + \mathbb{L}_\sigma(t) \tag{5}$$

where

$$\mathbb{L}_0 = \begin{pmatrix} 0 & 0 & -iJ & iJ \\ 0 & 0 & iJ & -iJ \\ -iJ & iJ & 0 & 0 \\ iJ & -iJ & 0 & 0 \end{pmatrix} \tag{6}$$

and

$$\mathbb{L}_\sigma = \begin{pmatrix} 0 & 0 & 0 & 0 \\ 0 & 0 & 0 & 0 \\ 0 & 0 & i[\sigma_1(t) - \sigma_2(t)] & 0 \\ 0 & 0 & 0 & -i[\sigma_1(t) - \sigma_2(t)] \end{pmatrix} \tag{7}$$

As the first step, we can define the equations of motion for the average, the zeroth-order moment,

$$\frac{\mathrm{d}\langle\hat{\rho}(t)\rangle}{\mathrm{d}t} = -\mathbb{L}_0\langle\hat{\rho}(t)\rangle - \langle\mathbb{L}_\sigma\hat{\rho}(t)\rangle \tag{8}$$

where

$$\langle\mathbb{L}_\sigma\hat{\rho}(t)\rangle = \begin{pmatrix} 0 & 0 & 0 & 0 \\ 0 & 0 & 0 & 0 \\ 0 & 0 & i[\langle\sigma_1(t)\rho_{12}(t)\rangle - \langle\sigma_2(t)\rho_{12}(t)\rangle] & 0 \\ 0 & 0 & 0 & -i[\langle\sigma_1(t)\rho_{21}(t)\rangle - \langle\sigma_2(t)\rho_{21}(t)\rangle] \end{pmatrix} \tag{9}$$

With the equality for the dichotomic process found by Bourret, Frisch, and Pouquet[23] for the independent dichotomic processes, the second-order moments can be factorized as $\langle\sigma_1(t)^2\rho_{ij}(t)\rangle = \Delta^2\langle\rho_{ij}(t)\rangle$, $\langle\sigma_2(t)^2\rho_{ij}(t)\rangle = \Delta^2\langle\rho_{ij}(t)\rangle$, $\langle\sigma_1(t)^2\sigma_2(t)\rho_{ij}(t)\rangle = \Delta^2\langle\sigma_2(t)\rho_{ij}(t)\rangle$, and $\langle\sigma_1(t)\sigma_2(t)^2\rho_{ij}(t)\rangle = \Delta^2\langle\sigma_1(t)\rho_{ij}(t)\rangle$, and Δ and ν are two parameters in the second-order time correlation function, $\langle\sigma_i(t)\sigma_i(0)\rangle = \Delta^2\exp(-\nu t)$ $(i = 1,2)$, of the dichotomic process.[23] We will discuss the Bourret equality as a good approximation for the independent Gaussian processes in section 3 in more detail. As a consequence of the Bourret equality, the moment space is reduced from infinity to 16

$$\begin{aligned}&(m_{11}^{0,0}, m_{22}^{0,0}, m_{12}^{0,0}, m_{21}^{0,0}, m_{11}^{1,0}, m_{22}^{1,0}, m_{12}^{1,0}, m_{21}^{1,0},\\ &m_{11}^{0,1}, m_{22}^{0,1}, m_{12}^{0,1}, m_{21}^{0,1}, m_{11}^{1,1}, m_{22}^{1,1}, m_{12}^{1,1}, m_{21}^{1,1})\end{aligned} \tag{10}$$

where $m_{ij}^{k_1,k_2} = \langle\sigma_1(t)^{k_1}\sigma_2(t)^{k_2}\rho_{ij}(t)\rangle$ and $k_1, k_2 \in \{0, 1\}$. Using the Shapiro and Loginov differentiation equation for the dichotomic process,

$$\begin{aligned}&\frac{\mathrm{d}}{\mathrm{d}t}\langle\sigma_1(t)^{k_1}\sigma_2(t)^{k_2}\rho_{ij}[t,\sigma_1(t),\sigma_2(t)]\rangle\\ &= -(k_1+k_2)\nu\langle\sigma_1(t)^{k_1}\sigma_2(t)^{k_2}\rho_{ij}[t,\sigma_1(t),\sigma_2(t)]\rangle\\ &\quad + \left\langle\sigma_1(t)^{k_1}\sigma_2(t)^{k_2}\frac{\mathrm{d}}{\mathrm{d}t}\rho_{ij}[t,\sigma_1(t),\sigma_2(t)]\right\rangle\end{aligned} \tag{11}$$

we obtain the equations of motion for the 16 moments. For $m_{ij}^{1,0}$, we have

$$\begin{aligned}\frac{\mathrm{d}}{\mathrm{d}t}m_{11}^{1,0} &= -\nu m_{11}^{1,0} - iJ(m_{21}^{1,0} - m_{12}^{1,0})\\ \frac{\mathrm{d}}{\mathrm{d}t}m_{22}^{1,0} &= -\nu m_{22}^{1,0} - iJ(m_{12}^{1,0} - m_{21}^{1,0}))\\ \frac{\mathrm{d}}{\mathrm{d}t}m_{12}^{1,0} &= -\nu m_{12}^{1,0} - iJ(m_{22}^{1,0} - m_{11}^{1,0}) - i\Delta^2 m_{12}^{0,0} + im_{12}^{1,1}\\ \frac{\mathrm{d}}{\mathrm{d}t}m_{21}^{1,0} &= -\nu m_{21}^{1,0} - iJ(m_{11}^{1,0} - m_{22}^{1,0})) - im_{21}^{1,1} + i\Delta^2 m_{21}^{0,0}\end{aligned} \tag{12}$$

for $m_{ij}^{0,1}$,

$$\begin{aligned}\frac{\mathrm{d}}{\mathrm{d}t}m_{11}^{0,1} &= -\nu m_{11}^{0,1} - iJ(m_{21}^{0,1} - m_{12}^{0,1})\\ \frac{\mathrm{d}}{\mathrm{d}t}m_{22}^{0,1} &= -\nu m_{22}^{0,1} - iJ(m_{12}^{0,1} - m_{21}^{0,1})\\ \frac{\mathrm{d}}{\mathrm{d}t}m_{12}^{0,1} &= -\nu m_{12}^{0,1} - iJ(m_{22}^{1,0} - m_{11}^{1,0}) - im_{12}^{1,1} + i\Delta^2 m_{12}^{0,0}\\ \frac{\mathrm{d}}{\mathrm{d}t}m_{21}^{0,1} &= -\nu m_{21}^{0,1} - iJ(m_{11}^{1,0} - m_{22}^{1,0})) - i\Delta^2 m_{21}^{0,0} + im_{21}^{1,1}\end{aligned} \tag{13}$$

and for $m_{ij}^{1,1}$,

$$\begin{aligned}\frac{\mathrm{d}}{\mathrm{d}t}m_{11}^{1,1} &= 2\nu m_{11}^{1,1} - iJ(m_{21}^{1,1} - m_{12}^{1,1})\\ \frac{\mathrm{d}}{\mathrm{d}t}m_{22}^{1,1} &= 2\nu m_{22}^{1,1} - iJ(m_{12}^{1,1} - m_{21}^{1,1})\\ \frac{\mathrm{d}}{\mathrm{d}t}m_{12}^{1,1} &= 2\nu m_{12}^{1,1} - iJ(m_{22}^{1,0} - m_{11}^{1,0}) - i\Delta^2 m_{12}^{0,1} + i\Delta^2 m_{12}^{1,0}\\ \frac{\mathrm{d}}{\mathrm{d}t}m_{21}^{1,1} &= 2\nu m_{21}^{1,1} - iJ(m_{11}^{1,0} - m_{22}^{1,0}) - i\Delta^2 m_{21}^{1,0} + i\Delta^2 m_{21}^{0,1}\end{aligned} \tag{14}$$

In total, we have 16 equations of motion from eqs 8, 12, 13, and 14. With the 16 equations, we can study the two-state non-Markovian open quantum systems. For the cases of dimeric and cyclic aggregates with 9 or 18 units driven by the dichotomic noise, several analytical and numerical studies on the influence of colored noise[28−30,30−33] have been carried out.

dx.doi.org/10.1021/jp111068w |J. Phys. Chem. B 2011, 115, 5499–5509

3. BOURRET APPROXIMATION

For the dichotomic process, the following equality holds

$$\langle x(t_i)x(t_{i-1})\Phi(t_{i-1})\rangle = \langle x(t_i)x(t_{i-1})\rangle\langle\Phi(t_{i-1})\rangle \quad (15)$$

due to the Bourret−Frisch−Pouquet theorem[23] and leads to its factorization of the multitime correlation function,

$$\begin{aligned}&\langle x(t_1)x(t_2)x(t_3)x(t_4)...x(t_{n-1})x(t_n)\rangle\\ &= \langle x(t_1)x(t_2)\rangle\langle x(t_3)x(t_4)\rangle...\langle x(t_{n-1})x(t_n)\rangle\end{aligned} \quad (16)$$

where $\Phi(t_{i-1})$ is an arbitrary functional of the dichotomic process. For the Gauss−Markov process, the multitime correlation function has the following recursive representation:

$$\begin{aligned}&\langle x(t_1)x(t_2)x(t_3)x(t_4)...x(t_{n-1})x(t_n)\rangle\\ &= \langle x(t_1)x(t_2)\rangle\langle x(t_3)x(t_4)...x(t_{n-1})x(t_n)\rangle\\ &+ \langle x(t_1)x(t_3)\rangle\langle x(t_2)x(t_4)...x(t_{n-1})x(t_n)\rangle + ...\\ &+ \langle x(t_1)x(t_n)\rangle\langle x(t_2)x(t_3)...x(t_{n-2})x(t_{n-1})\rangle\end{aligned} \quad (17)$$

The equations of motion of moments for the SLE driven by the Gauss−Markov process form an infinite set of linear equations;[26] i.e., the linear moment space is infinite. A truncation scheme is inevitable to solve the infinite linear dynamical system. The simplest one is using the Bourret equality as an approximation because the equations of motions of the zeroth- and first-order moments defined in eqs 8, 12, 13, and 14 are the same for the SLEs driven by the dichotomic and Gauss−Markov processes. Numerically, we can consider the dichotomic process a coarse-grained representation of the Gaussian process. We should stress here that the way to use the Bourret approximation is different and better than the way used in the Bourret integral equation (and its corresponding quantum master equation, Redfield equation) because we have the correct time ordering in the generation of the equations of motions of moments. As a result, we can study the dynamics of the excitation energy transfer in multichromophoric systems with exponentially correlated non-Markovian random Gaussian noise using eqs 21 and 23. Previous studies of electron or exciton transport show that the dichotomic process and the Gauss−Markov process with the same parameters agree with each other reasonably well for the diffusion constants, in the linear lattice and square lattice models, for intermediate damping.[12,34] The possible difference between the dichotomic and Gauss−Markov processes with the same parameters will not be the topic of this paper. Further numerical simulation results will be able to give us an idea of how valid this truncation scheme will be. As the only explicit and exactly non-Markovian model available to us, eqs 8, 12, 13, and 14 and the general ones, eqs 21 and 23, will provide insight about the non-Markovian dynamics. We will present the results for symmetric dimers in section 4 and have more discussion there. The details of the statistical properties of the Gauss−Markov and dichotomic processes are discussed in Appendix B.

In the limit of the white noise, the dichotomic and Gauss−Markov processes converge to each other[35] to be Gaussian white noise. For Gaussian white noise, the factorization of the multitime correlation function can be expressed as

$$\begin{aligned}&\langle x(t_0)x(t_1)x(t_2)x(t_3)...x(t_{n-1})x(t)\rangle\\ &= (2\lambda)^n\delta(t_n - t_{n-1})...\delta(t_4 - t_3)\delta(t_2 - t_1)\end{aligned} \quad (18)$$

due to the following relationship

$$\lim_{\nu\to\infty} \Delta^2 \exp[-\nu(t_i - t_{i-1})] = 2\lambda\delta(t_i - t_{i-1}) \quad (19)$$

where $\lambda = \lim_{\nu\to\infty}(\Delta^2/\nu)$, and $\nu \exp[-\nu(t_i - t_{i-1})] = 2\delta(t_i - t_{i-1})$. Although it appears that the multitime correlation function does not have the Gaussian property in the summation over the different permutations of time variables, as appears in the general form for the Gaussian process in eq 17, only one term contributes for a specific time ordering, due to the exact delta correlation.[36] The Gaussian white noise is equivalent to the Ornstein−Uhlenbeck process or the dichotomic process with zero correlation time and infinite variance. The factorizations shown in eqs 16 and 18 are the basic reason why we can solve the Haken−Strobl−Reineker model and the SLE driven by the dichotomic processes analytically.

4. NON-MARKOVIAN EFFECT, LOCALIZATION, AND MOTIONAL NARROWING IN SYMMETRIC DIMER

The different master equations based on the techniques of either cumulant expansion or projection operator with the second-order truncation have been successfully[6−8,11,18] used to study the line shape and transport for excitons with dynamic disorder with weak fluctuation damping or short correlation time (essentially small Kubo number). In this section, we will apply this non-Markovian SLE model to the study of non-Markovian effects in the symmetric dimer. The simulation results show that the non-Markovian effect is quite complicated and has a significant impact on the population dynamics of excitation energy transfer. Motional narrowing and localization are observed in the limits of the fast fluctuations and slow fluctuations (static disorder). In the larger Kubo number region, i.e., the region of strong damping and long correlation time, the simulation results show that the second-order master equation approach is not sufficient to describe the non-Markovian effect. Furthermore, implications in the transfer efficiency of the excitation energy transfer in the FMO complex will be discussed in section 5.

In order to systematically illustrate the non-Markovian effect, we will look at the three cases weak damping, intermediate damping, and strong damping for $J = 1$:

- weak damping region, $\Delta^2 = 0.1$,
- intermediate damping region, $\Delta^2 = 1$,
- strong damping region, $\Delta^2 = 20$.

And we choose the nonequilibrium initial condition to be

$$\rho(0) = \begin{pmatrix} 1/3 & \sqrt{2}/3 \\ \sqrt{2}/3 & 2/3 \end{pmatrix}$$

In each case, we will consider four different ν's, $\nu = 0.1$, 1, 10, and 100. For the weak damping case, the plotted results are shown in Figure 1; for the intermediate damping case, the plotted results are shown in Figure 2; and for the strong damping case, the plotted results are shown in Figure 3.

For the symmetric dimer, in the second cumulant expansion, the population decay rate[8,11] can be expressed as $\Gamma \approx \Delta^2\nu/(\nu^2 + J^2)$. The formula is valid for weak fluctuation damping and short correlation time (essentially small Kubo number).[37] The J-scaled Γ

$$\frac{\Gamma}{J} = \frac{\Delta^2}{J}\frac{\nu}{\nu^2 + J^2} \quad (20)$$

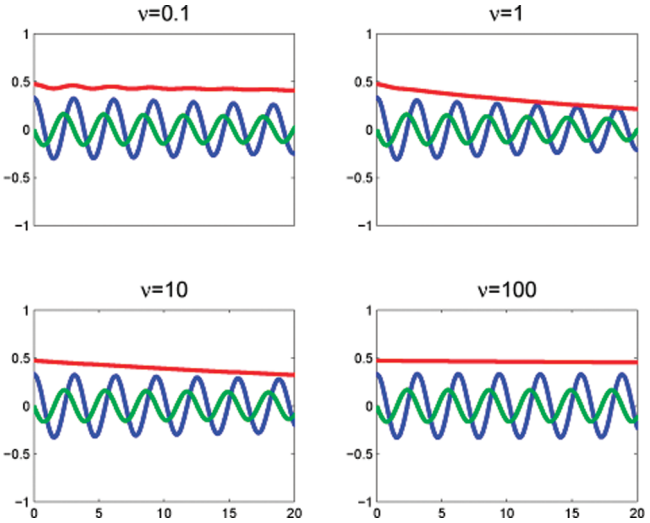

Figure 1. Case 1, weak damping: $\Delta^2 = 0.1$ and $J = 1$. The blue solid line represents the population difference of site 1 and site 2 $(\rho_{22} - \rho_{11})$; the red solid line represents the real part of coherence, ρ_{12}; the green solid line represents the imaginary part of coherence, ρ_{12}. The four panels correspond to four different ν's, ν = 0.1, 1, 10, and 100.

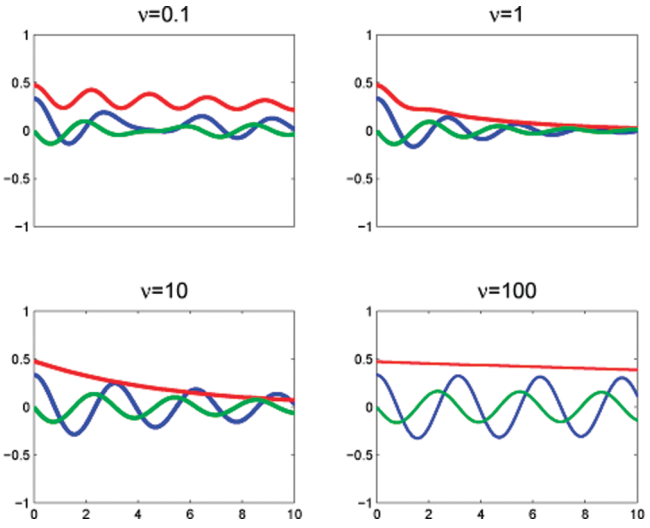

Figure 2. Case 2, intermediate damping: $\Delta^2 = 1$ and $J = 1$. The blue solid line represents the population difference of site 1 and site 2 $(\rho_{22} - \rho_{11})$; the red solid line represents the real part of coherence, ρ_{12}; the green solid line represents the imaginary part of coherence, ρ_{12}. The four panels correspond to four different ν's, ν = 0.1, 1, 10, and 100.

is associated with the coherent motion of populations. When $(\Gamma/J) > 1$, coherent motion will disappear. The formula also shows that there is a maximum relaxation rate at $\nu = J$. The results in Figures 1 and 2 confirm that, when $\nu = J$, the relaxation rate Γ is approximately the largest as predicted by eq 20. However, in Figure 3 (strong damping case), no maximum at $\nu = J$ can be found, since the validity of the formula defined in eq 20 does not hold in this case. Figure 2 seems to show that the formula can even work for the intermediate damping case. In the symmetric dimer, the exciton energy difference is $2J$ and the phonon bandwidth is $2\nu_i$ as defined in the Lorentzian spectral density used in subsection 5.1. This intriguing result suggests that only when the phonon bandwidth is equal to the exciton energy

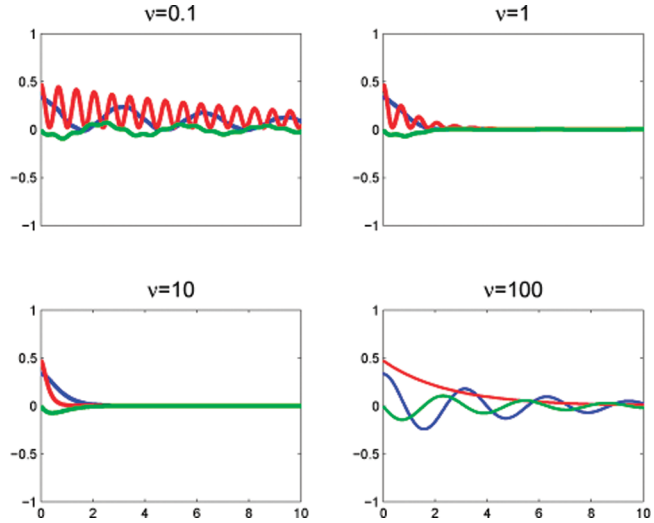

Figure 3. Case 3, strong damping: $\Delta^2 = 20$ and $J = 1$. The blue solid line represents the population difference of site 1 and site 2 $(\rho_{22} - \rho_{11})$; the red solid line represents the real part of coherence, ρ_{12}; the green solid line represents the imaginary part of coherence, ρ_{12}. The four panels correspond to four different ν's, ν = 0.1, 1, 10, and 100.

difference is the relaxation of the excitation energy the most effective in destroying the coherence. This dynamical phenomena can be explained by the overlap of the phonon bands of the two sites. If the bandwidth is extremely narrow, i.e., ν is extremely small, then there is no overlap at all. As a result, no incoherent transfer is possible through the phonon bands. In the case of $\nu = J$, where the two symmetric phonon bands have the half-overlap, the decay process through the incoherent phonon channel is the strongest. If the phonon bandwidth is extremely broad, i.e., ν is extremely large, then the two bands are perfectly overlapped with each other, which corresponds to the fast modulation limit. Since the depth for the broad phonon band is very small and proportional to $1/\nu$, it is hard to transfer energy incoherently through the phonon, and coherence can be preserved.

For the cases with either weak coupling or short correlation time, we can claim that, when $(\Gamma/J) > 1$, the coherent motion of the population will disappear. However, as shown in Figure 3, the prediction of the disappearance of coherent motions of populations when $(\Gamma/J) > 1$ fails for $\nu = 0.1$ (long correlation time and strong coupling). The corresponding Kubo number (Δ/ν) case is equal to $10 \times (20)^{1/2} \gg 1$, which is the reason why the prediction fails. For the non-Markovian model driven by the dichotomic or Gauss−Markov process, the Kubo number is a more rigorous criterion to guarantee the validity of the second-order master equation.[37]

Figures 1 and 3 consistently show that, when ν is large, i.e., the correlation time is small (fast modulation limit), relaxation is slowed down due to motional narrowing and, when ν is small, i.e., the correlation time is large, relaxation is also slowed down due to localization. The three figures also show that, in the motional narrowing limit, the real part of the coherence, $real(\rho_{12})$, is not oscillatory. However, in the localization limit, the real part is oscillatory as long as the populations, ρ_{11} and ρ_{22}, survive and oscillate. Since the exciton population is connected to $real(\rho_{12})$, our plotted results confirm that the long correlation time (or small ν) will lead to exciton population oscillation. However, the exciton population oscillation will not be observed when the

dx.doi.org/10.1021/jp111068w |J. Phys. Chem. B 2011, 115, 5499–5509

fluctuation rate, ν, is very large. When $\nu \rightarrow 0$, the correlation time goes to infinity, we approach the limit of static disorder.

5. CORRELATION TIME AND EXCITATION ENERGY TRANSFER IN THE FMO COMPLEX

Both diagonal and off-diagonal energetic disorders are observed in the different experiments in multichromophoric light harvesting systems.[38,39] In subsection 5.1, we will show how to determine the two parameters, Δ and ν, from the Frenkel exciton Hamiltonian.[40] For the purpose of simplification, we only consider the interacting chromophoric systems in the FMO complex with diagonal disorder only; i.e., $\sigma(t)$ is diagonal and $\langle \sigma_{i_1 j_1}(t_1)\sigma_{i_2 j_2}(t_2)\rangle = \Delta_{i_1 j_1}{}^2 \exp(-\nu(t_2 - t_2))\delta_{i_1 i_2}\delta_{j_1 j_2}$ for $t_2 > t_1$. It is easy to include off-diagonal disorder in the same fashion.

5.1. Frenkel Exciton Hamiltonian and Parametrization of Dichotomic and Gaussian Processes. In order to model the excitation energy transfer with our current non-Markovian model, we need to parametrize the dichotomic and Gauss−Markov processes by determining ν and Δ^2. They can be obtained by fitting experimental data[41] or calculated theoretically from the Frenkel exciton Hamiltonian in the high temperature limit. As used in ref 42, the Hamiltonian is expressed as

$$H = H^{\mathrm{el}} + H^{\mathrm{ph}} + H^{\mathrm{reorg}} + H^{\mathrm{el-ph}}$$

where

$$H^{\mathrm{el}} = \sum_{i=1}^{N} |i\rangle\varepsilon_i\langle i| + \sum_{i=1}^{N}\sum_{j=i+1}^{N} J_{ij}(|i\rangle\langle j| + |j\rangle\langle i|)$$

$$H^{\mathrm{ph}} = \sum_{i=1}^{N} H_i^{\mathrm{ph}}$$

$$H^{\mathrm{reorg}} = \sum_{i=1}^{N} |i\rangle\lambda_i\langle i|$$

and

$$H^{\mathrm{el-ph}} = \sum_{i=1}^{N} H_i^{\mathrm{el-ph}} = \sum_{i=1}^{N} V_i\mu_i$$

where μ_i is a phonon operator on site i, V_i a system operator, and only the diagonal exciton−phonon coupling is considered.

According to the quantum fluctuation−dissipation[43−45] relation,

$$S_i(t) = \frac{1}{2}\langle[\mu(t),\mu(0)]_+\rangle_{\mathrm{ph}}$$

$$\chi_i(t) = \mathbf{i}\langle[\mu(t),\mu(0)]_-\rangle_{\mathrm{ph}}$$

$$\langle\mu_i(t)\mu_i(0)\rangle = S_i(t) - \mathbf{i}\chi_i(t)/2$$

where

$$S_i(t) = \frac{1}{\pi}\int_0^\infty \mathrm{d}\omega\chi_i''(\omega)\coth\frac{\beta\omega}{2}\cos\omega t$$

$$\chi_i(t) = \frac{2}{\pi}\int_0^\infty \mathrm{d}\omega\chi_i''(\omega)\sin\omega t$$

we take $\chi_i''(\omega) = 2\lambda_i(\omega\nu_i/(\omega^2+\nu_i^2))$ and $\chi_i(\omega) = \int_0^\infty \mathrm{d}t\mathrm{e}^{i\omega t}\chi_i(t)$. At high temperature, $S_i(t) \approx (2\lambda_i/\beta)\mathrm{e}^{-\nu_i t}$, $\chi_i(t) = 2\lambda_i\nu_i e^{-\nu_i t}$ for the Drude−Lorentz phonon spectral density. According to the above definition, ν_i is a measure of the phonon bandwidth at site i. As a result, the time correlation functions for the dichotomic and Gauss−Markov processes can be defined by dropping the imaginary part, $\chi_i(t)$, when $(1/\beta) \gg \nu_i$ in the high temperature limit and only keeping the real part $S_i(t)$. Corresponding to our notation, $\Delta_{ii}{}^2 = 2\lambda_i/\beta$ and $\nu_{ii} = \nu_i$. Quantum temperature corrections can be done partially by including $\chi_i(t) = 2\lambda_i\nu_i e^{-\nu_i t}$ and expanding the dichotomic and Gauss−Markov processes to be complex-valued,[46] where $\Delta_{ii}{}^2 = (2\lambda_i/\beta) - i\lambda_i\nu_i$.

This parametrization of the dichotomic and Gauss−Markov processes should be fully valid in the high temperature limit. The exact treatment of quantum fluctuations needs to take into consideration the time ordering, non-Markovian, and detailed balance for the quantum process of the phonon bath at the low temperature. The current existing quantum mechanical methods[47−50] based on the real time path integral formalism are limited to the spin-boson (dimer) model. Solving the general exciton−phonon (multichromophore) Hamiltonian exactly is still an open theoretical problem. Therefore, our non-Markovian model is valuable because it is exactly solvable and we can study non-Markovian quantum dynamics in a multichromophoric system. The quantum temperature correction is possible and some schemes have been proposed.[18,51,52]

5.2. Excitation Energy Transfer in the FMO Complex. The FMO complex, as a simple realistic model system, has been extensively studied experimentally and theoretically.[1,40,53−56] The Hamiltonian describing the single excitation in the FMO complex from ref 40 is used. As already pointed out, we only consider diagonal fluctuations, $\sigma_{ii}(t)$, in eqs 21 and 23. We assume that ν_{ii} and Δ_{ii} are the same for all the sites for simplicity. Given this assumption, we will use Δ and ν to replace Δ_{ii} and ν_{ii} for the rest of the paper. Different Δ and ν for different sites can be implemented easily in our model, which is the advantage of this model and will be useful to study the individual local site environmental effect. Since Engel and Fleming's experiments of the FMO complex[1,56] have been done at two temperatures, 77 and 300 K, we will implement the non-Markovian model to simulate the FMO complex system at these temperatures. Using the results of Section 5.1, we estimate the parameters of the dichotomic and Gauss−Markov processes from the spectral density and reorganization energy suggested in the same reference mentioned earlier. Figure 4 shows the plotted results of the population dynamics in the FMO complex at 77 K, where the correlation time is τ_c = 50 fs and reorganization energy is equal to 35 cm^{-1}. Figures 5 and 6 show the plotted results of population dynamics at 300 K, where the correlation times are τ_c = 50 and 166 fs and the reorganization energy is equal to 35 cm^{-1}. We can see our non-Markovian model provides results similar to the recent experimental results. We can see the population coherent motion can last for 1000 fs in Figure 4, 600 fs in Figure 5, and around 1000 fs in Figure 6.

In the non-Markovian model, ν_{ii} (the inverse of the correlation time) is proportional to the phonon bandwidth, as shown in section 5.1. It implies that the protein environment could protect the coherence of the exciton transfer and speed up the exciton transfer by adjusting the phonon bandwidth. However, this hypothesis needs more computational and experimental support. We will discuss the efficiency of the transfer in the next section and partially uncover the role of ν_{ii} in the transfer efficiency with our non-Markovian model.

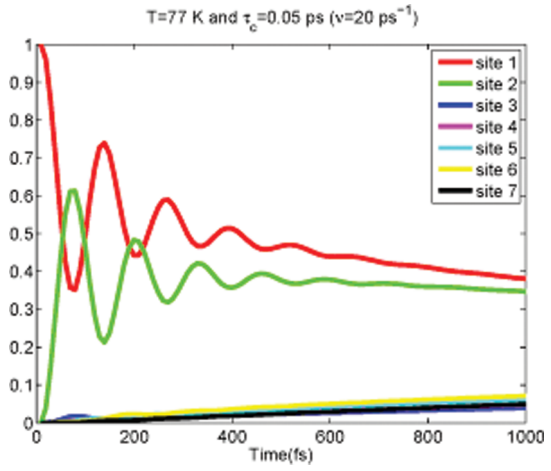

Figure 4. The population dynamics in the seven sites shown at a temperature of $T = 77$ K. The reorganization energy is equal to 35 cm^{-1}, and the correlation time is $\tau_c = 50$ fs.

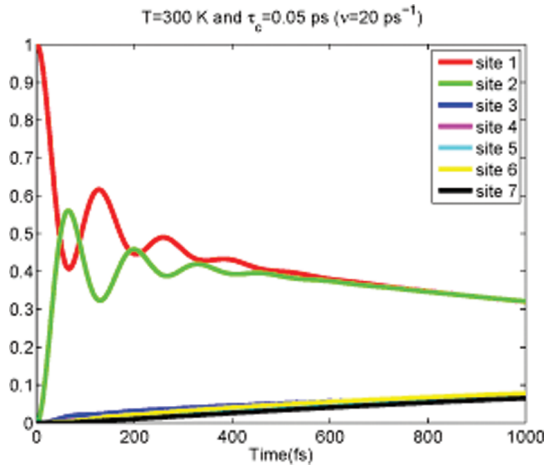

Figure 5. The population dynamics in the seven sites shown at a temperature of $T = 300$ K. The reorganization energy is equal to 35 cm^{-1}, and correlation time is $\tau_c = 50$ fs.

Thanks to the structure of the dichotomic process, we can obtain the master equation for excitons, ρ^{ex}, by rotating the Hamiltonian from the local basis to the exciton basis as we did for the generalized Haken−Strobl−Reineker model.[3] Figures 7 and 8 show the evolution of excitons with the same initial conditions, correlation time, and reorganization energy as used in Figures 4 and 5. We can clearly see the oscillation of exciton populations, especially at 77 K. The time evolution of the 1−3 exciton coherence at the temperatures 77 and 300 K is shown in Figures 9 and 10.

5.3. Narrowing, Mean First Passage Time (FPT), and Transfer Efficiency. Recent theoretical study in the FMO complex network shows that fluctuations (noise) can enhance the excitation energy transfer efficiency.[57−60] The models used to address the efficiency question, such as the Redfield and Lindblad equations, have ignored the non-Markovian effect by assuming the Markovian limit in the second-order master equation.[61,62] Fan and co-workers[63] have used the Debye spectral density to treat non-Markovian effects based on the COP second-order master equation to give a semiquantitative description of the non-Markovian

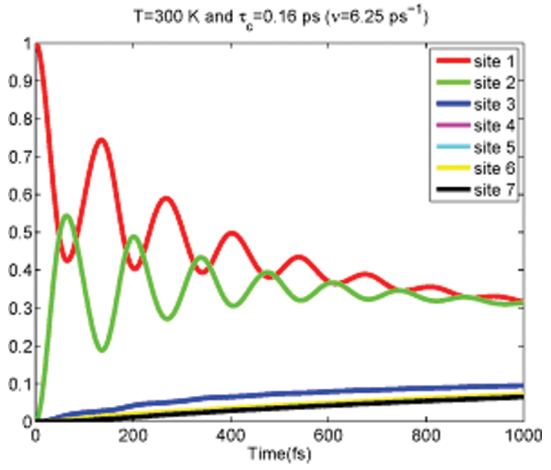

Figure 6. The population dynamics in the seven sites shown at a temperature of $T = 300$ K. The reorganization energy is equal to 35 cm^{-1}, and the correlation time is $\tau_c = 166$ fs.

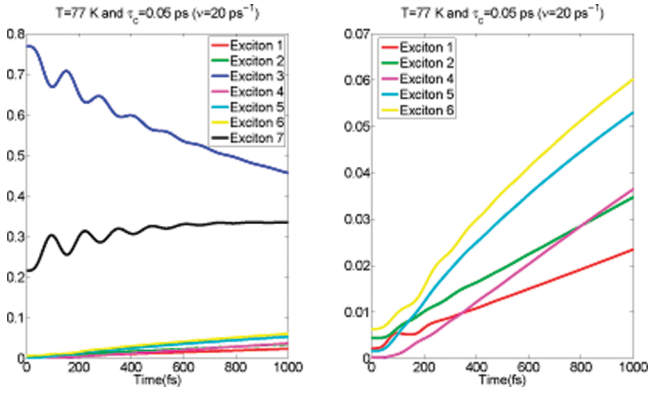

Figure 7. The population dynamics of excitons shown at a temperature of $T = 77$ K. The reorganization energy is equal to 35 cm^{-1}, and the correlation time is $\tau_c = 50$ fs. The left panel shows the dynamics of all seven excitons; the right panel shows the close-ups of the time trajectories of excitons 1, 2, 4, 5, and 6.

effect. In this section, we will show how the transfer efficiency is affected by Δ (or essentially, the reorganization energy for a constant temperature) and the rate ν.

We take the definition of the efficiency of excitation energy transfer based on the quantum trapping yield.[64] Given a fixed trapping rate and very small decay rate, the efficiency is inversely proportional to the mean FPT $\langle t \rangle$. Within our non-Markovian model, we phenomenologically consider the trapping rate to be 1 ps^{-1}.[65] In this paper, we chose the initial condition to be $\rho_{11}(0) = 1$ in the site basis and other populations $\rho_{nn}(0)$ are zero. However, calculation results not reported in this paper show that the efficiency of the FMO excitation energy transfer network is not particularly sensitive to the initial condition when there is noise.

The role of the correlation time, $\tau_c = 1/\nu$, due to phonons is important in transfer efficiency. The reason is twofold. One is that the long correlation time will protect the coherence and enhance the excitation energy transfer through the quantum coherence. However, if the correlation time is too long, the excitation energy will be localized (localization by static disorder) and the transfer efficiency will be diminished. The other reason is

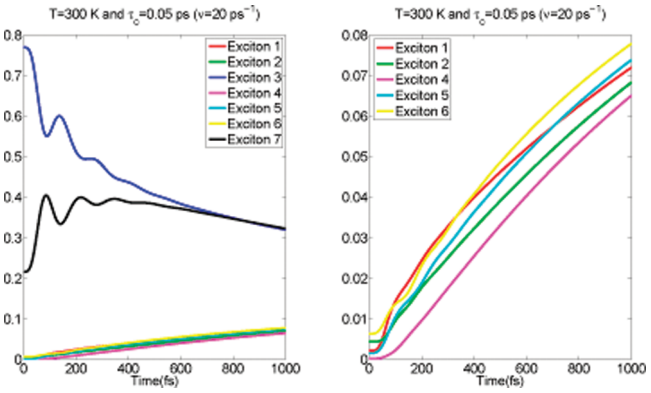

Figure 8. The population dynamics of excitons shown at a temperature of T = 300 K. The reorganization energy is equal to 35 cm^{-1}, and the correlation time is τ_c = 50 fs. The left panel shows the dynamics of all seven excitons; the right panel shows the close-ups of the time trajectories of excitons 1, 2, 4, 5, and 6.

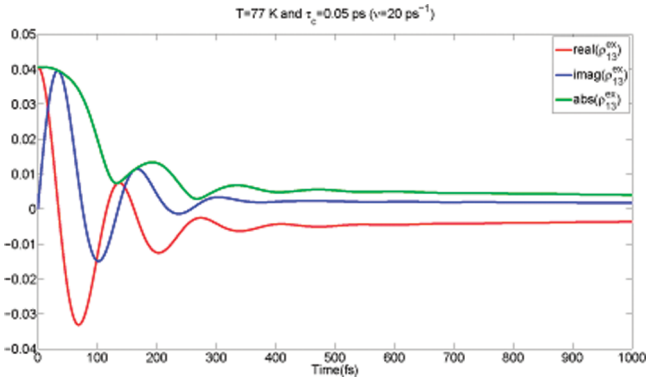

Figure 9. The time trajectories of the real part (solid red line), imaginary part (solid blue line), and absolute value (solid green line) of the 1−3 exciton coherence, ρ_{13}^{ex}, shown at a temperature of T = 77 K. The reorganization energy is equal to 35 cm^{-1}, and the correlation time is τ_c = 50 fs.

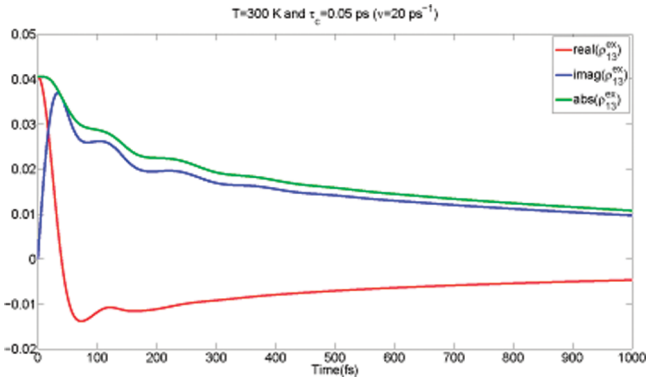

Figure 10. The time trajectories of the real part (solid red line), imaginary part (solid blue line), and absolute value (solid green line) of the 1−3 exciton coherence, ρ_{13}^{ex}, shown at a temperature of T = 300 K. The reorganization energy is equal to 35 cm^{-1}, and the correlation time is τ_c = 50 fs.

that, when the fluctuation is too fast, the motional narrowing effect will preserve the coherence of the excitation energy. As a result, the energy is not transferred to the trapping site efficiently either, because some of the exciton states are orthogonal to the trap.

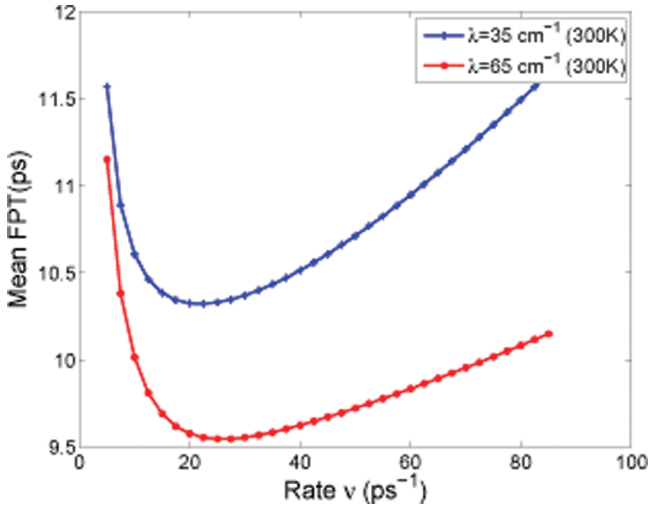

Figure 11. Mean FPT vs ν. The blue line shows the plotted result of a reorganization energy equal to 35 cm^{-1}, and the red line shows the plotted result of a reorganization energy equal to 65 cm^{-1}.

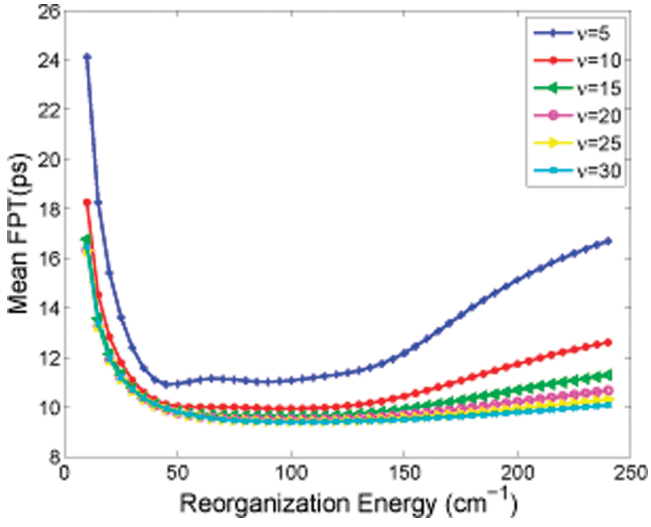

Figure 12. Mean FPT vs reorganization energy. The colors represent six different ν's. The blue line represents ν = 5 ps^{-1}, the red line ν = 10 ps^{-1}, the green ν = 15 ps^{-1}, the pink ν = 20 ps^{-1}, the yellow ν = 25 ps^{-1}, and the sky blue ν = 30 ps^{-1}.

In Figure 11, we show the results of mean FPT vs ν at 300 K. Clearly, we can see that, when ν is extremely large or small for two values of reorganization energy, the mean FPT will increase and the transfer efficiency will diminish. When the reorganization energy is equal to 65 cm^{-1}, the ν corresponding to the minimum mean FPT is equal to 20 ps^{-1}; when the reorganization energy is equal to 35 cm^{-1}, the ν corresponding to the minimum mean FPT is slightly larger than 20 ps^{-1}. These results show that ν = 20 ps^{-1} approximately is an optimal rate or 50 fs is an optimal correlation time for the optimally efficient energy transfer.

Figure 12 presents the relationship between reorganization energy and energy transfer efficiency. It is clearly shown that, when ν increases from ν = 5 ps^{-1} to ν = 30 ps^{-1}, the flat region gets larger. In other words, a larger ν will make the energy

dx.doi.org/10.1021/jp111068w |J. Phys. Chem. B 2011, 115, 5499–5509

transfer efficiency less sensitive to the reorganization energy change. Also when $\nu > 10$ ps^{-1}, the difference of curves for different ν's is very small. At $\nu = 5$, there is a small local maximum in which the reorganization energy is around 75 cm^{-1}. This could be due to the localization at relatively fast fluctuation,[34] and it needs more study to identify its origin.

Combining the plotted results of Figures 11 and 12, the following conclusion can be made: if reorganization energy is roughly within the range between 35 and 150 cm^{-1}, the optimal rate ν should fall into a small interval around 20 ps^{-1}, or the correlation time in a small interval around 50 fs. More specifically, the optimal correlation time is within a small interval around 20 ps^{-1} for a broad range of reorganization energy at $T = 300$ K. Our model also suggests that the non-Markovian effect can make the optimal energy transfer efficiency quite robust and insensitive to reorganization energy ranging from 35 to 150 cm^{-1}, as shown in Figure 12.

6. CONCLUDING REMARKS

In this paper, we introduced an exactly solvable SLE driven by the dichotomic process to study the non-Markovian effect in excitation energy transfer. The Shapiro and Loginov differentiation formula provides a simple but powerful mathematical tool to solve any SLE whose random coefficients are governed by the Fokker−Planck equation. For the SLE driven by the dichotomic process, we can generate a set of equations of motion of moments. Since the SLEs driven by the dichotomic and Gaussian processes with the same parameters, Δ and ν, have the same equation of motion for the first-order moment, we can use the Bourret approximation as a simple truncation scheme to study the SLE driven by the Gaussian process. With the same parameters, previous studies in exciton and electron transports show that the SLE driven by the dichotomic process is a good approximation to that driven by the Gaussian process.

With the SLE model, we studied the non-Markovian effect in the symmetric dimer. We found that there is a maximum population relaxation rate equal to J which is predicted in refs 8 and 11. The results in section 4 show that, when the time correlation is large or damping is large, the second-order master equation can fail to describe the non-Markovian effect. Localization and motional narrowing are observed for a variety of damping strengths.

We applied the non-Markovian SLE model to study the excitation energy transfer in the FMO complex. Parameterizing the dichotomic and Gaussian processes according to the Frenkel exciton Hamiltonian, we simulated the population dynamics for the FMO complex in the site basis. We can see that the coherent motion of populations in the FMO complex lasts for 600−1000 fs for $T = 77$ K with $\nu = 20$ ps^{-1}and $T = 100$ K with $\nu = 20$ ps^{-1} and $\nu = 6.25$ ps^{-1}, which well agree with the recent study given that we have a relatively simple model. On the basis of the definition of energy transfer efficiency by Cao and Silbey,[64] we look at the time correlation and damping (reorganization energy) effects on the energy transfer in the FMO complex. It is found that neither the long nor the short correlation time is optimal for the energy transfer efficiency due to the localization and motional narrowing. The SLE model also shows that transfer efficiency has an optimal correlation time in the small interval around 50 fs for a broad range of reorganization energies, which can be partially attributed to the robustness of the FMO energy transfer network.

We used the SLE to study the fast dynamics in the light harvesting systems. The two model systems of the dimer and FMO complex are used in this paper to address different effects due to a phonon bath. As discussed in section 5.1, the high temperature limit of the SLE leads to the equal distribution of site energy populations. Future work will be focused on extending the current model to take into account the effect of temperature using a harmonic oscillator (phonon) quantum bath that will provide the correct description of the long-time equilibrium of the electronic excitation energy transfer system.

APPENDIX A. MULTICHROMOPHORIC SYSTEMS AND GENERALIZED EQUATIONS OF MOTION OF MOMENTS

As defined in eq 5, for the general case, $\mathbb{L}_0 = i[H_0, \cdot\,]$ and $\mathbb{L}_\sigma(t) = i[\sigma(t), \cdot\,]$, where we assume that H_0 and $\sigma(t)$ are full matrices and the matrix elements in $\sigma(t)$ are independent dichotomic. Applying eq 11, we have the following equations of motion of moments for the general cases:

$$\frac{d}{dt} m_{ij}^{0,0,\ldots,0} = -i \sum_l [(H_0)_{il} m_{lj}^{0,0,\ldots,0} - (H_0)_{lj} m_{il}^{0,0,\ldots,0}] \tag{21}$$

$$- i \sum_l (m_{lj}^{0,\ldots,\overset{il}{1},\ldots,0} - m_{il}^{0,\ldots,\overset{lj}{1},\ldots,0}) \tag{22}$$

where the overscripts il and lj point to the corresponding matrix elements of $\sigma(t)$ with the exponent equal to 1, and

$$\begin{aligned} \frac{\mathrm{d}}{\mathrm{d}t} m_{ij}^{k_{11}, k_{12}, \ldots, k_{nn}} &= - \sum_{l,m=1}^{N} k_{lm} \nu_{lm} m_{ij}^{k_{11}, k_{12}, \ldots, k_{nn}} \\ &- i \sum_{l=1}^{N} [(H_0)_{il} m_{lj}^{k_{11}, k_{12}, \ldots, k_{lj}, \ldots, k_{nn}} - (H_0)_{lj} m_{il}^{k_{11}, k_{12}, \ldots, k_{il}, \ldots, k_{nn}}] \\ &- i \sum_{l}^{N} [\delta_{k_{il}1} {\Delta_{il}}^2 m_{lj}^{k_{11}, k_{12}, \ldots, \overset{il}{0}, \ldots, k_{nn}} - \delta_{k_{lj}1} {\Delta_{lj}}^2 m_{il}^{k_{11}, k_{12}, \ldots, \overset{lj}{0}, \ldots, k_{nn}}] \\ &- i \sum_{l}^{N} [\delta_{k_{il}0} m_{lj}^{k_{11}, k_{12}, \ldots, \overset{il}{1}, \ldots, k_{nn}} - \delta_{k_{lj}0} m_{il}^{k_{11}, k_{12}, \ldots, \overset{lj}{1}, \ldots, k_{nn}}] \end{aligned} \tag{23}$$

where N is the number of chromophores, $m_{ij}^{k_{11},k_{12},\ldots,k_{lm}\ldots k_{nn}} = \langle \sigma_{11}(t)^{k_{11}} \sigma_{12}(t)^{k_{12}} \ldots \sigma_{lm}(t)^{k_{lm}} \ldots \sigma_{nn}(t)^{k_{nn}} \rho_{ij}(t) \rangle$, $\sigma_{lm}(t)$ is the dichotomic process, and k_{lm} is the exponent and takes the values of $\{0, 1\}$ because of the Bourret−Frisch−Pouquet theorem[23]

$$\langle \sigma_{lm} m_{ij}^{k_{11}, k_{12}, \ldots, \overset{lm}{1}, \ldots, k_{nn}} \rangle = {\Delta_{lm}}^2 m_{ij}^{k_{11}, k_{12}, \ldots \overset{lm}{0}, \ldots, k_{nn}}$$

The procedure defined in eqs 21 and 23 leads to $N^2 \times 2^{N \times N}$ equations of motion of moments when $\sigma(t)$ is a full matrix. If $\sigma(t)$ is a diagonal matrix, i.e., we only consider the diagonal disorder and dephasing in the dynamics, the dimensionality of the question will be reduced to $N^2 \times 2^N$. Obviously, the set of equations of motion has bad exponential scaling. For some symmetries, the number of the linear differential equations of moments can be reduced significantly.[66] Numerically, for multichromophoric systems with less than 10 chromophores and diagonal disorder only, this exact model is still manageable, e.g., the FMO complex with seven sites. We show the simulation results for the FMO complex in section 5.

APPENDIX B. STATISTICAL PROPERTIES OF GAUSS−MARKOV PROCESS AND DICHOTOMIC PROCESS

The Gaussian process is a continuous time continuous state random process. The Gaussian process[67,68] can be constructed as a continuous limit of the discrete-time random process with the joint probability distribution function (PDF),

$$p(x_0, x_1, x_2, \dots, x_n) = \frac{1}{\sqrt{2\pi M}} \exp\left\{-\frac{1}{2}\sum_{i,j=0}^{n} x_i (M^{-1})_{ij} x_j\right\} dx_0\, dx_1\, dx_2 \dots dx_n \quad (24)$$

on the time lattice $\{t_0, t_1, t_2, \dots, t_{n-1}\}$, where $x_n = x(t)$, $x_i = x(t_i)$, $M_{ij} = \langle x(t_i)x(t_j)\rangle$, and $i, j = 0, 1, \dots, n$. Since the matrix element of M is only dependent on the time difference, the joint PDF defines a stationary non-Markov Gaussian process. Once we have the joint PDF, the general moment generating function or general characteristic function can be defined and provides the same information of the joint PDF.

For the stationary Gauss−Markov process,[67] the Ornstein−Uhlenbeck process is the only implementation based on Doob's theorem. Given the Markov property of the process, the inverse of covariance matrix M will be tridiagonal; i.e., the joint PDF can be expressed as

$$p(x_0, x_1, x_2, \dots, x_n) = p(x_0)P(x_1|x_0)P(x_2|x_3)\dots P(x_n|x_{n-1}) \quad (25)$$

where

$$P(x_i|x_{i-1}) = \frac{1}{\sqrt{2\pi\Delta(1 - r_{i-1}{}^2)}} \exp\left[-\frac{(x_i - r_{i-1}x_{i-1})^2}{2\Delta(1 - r_{i-1}{}^2)}\right]$$

and $r_{i-1} = \exp[-\nu(t_i - t_{i-1})]$ and otherwise 0. With the above joint PDF, the multitime correlation function identity in eq 17 can be recovered.

The dichotomic process, as a two-state Markov process, the joint PDF on the discrete time lattice can be expressed as

$$p(x_0, x_1, x_2, \dots, x_n) = p(x_0)P(x_1|x_0)P(x_2|x_1)\dots P(x_n|x_{n-1})$$

where $x_i = \{a_1, a_2\}$, the two states and the transition probability matrix are given as

$$P(x_i|x_{i-1}) = \frac{1}{\nu_1 + \nu_2}\begin{pmatrix} \nu_1 & \nu_1 \\ \nu_2 & \nu_2 \end{pmatrix} + \frac{1}{\nu_1 + \nu_2}\begin{pmatrix} \nu_2 & -\nu_1 \\ -\nu_2 & \nu_1 \end{pmatrix} \exp[-(\nu_1 + \nu_2)(t_i - t_{i-1})]$$

and $p(x_0)$ is the initial probability of $x_0 = a_1$ or $x_0 = a_2$. The dichotomic process is the special case of the two-state Markov process with the equalities $\nu_1 = \nu_2$ and $a_1 = -a_2$. Mathematically, the Gauss−Markov process can be considered as the continuous state generalization of the dichotomic process. However, the critical difference between the Gauss−Markov and dichotomic processes is that the transition probability, $P(x_i|x_{i-1})$, of the Gauss−Markov process has a dependence on the current value, x_{i-1}; for the dichotomic process, the transition probability is independent of the current value, x_{i-1}.

The connection between the dichotomic process and the Gauss−Markov process is deeply reflected in the following expression:[26]

$$\alpha(t) = \sum_{k=1}^{N} \beta_k(t) \quad (26)$$

where $\beta_k(t)$ is an independent and identically distributed dichotomic random variable and $\alpha(t)$ will approach the Ornstein−Uhlenbeck random variable when $N \to \infty$ as a result of the central limit theorem. The convergence rate of the summation to the OU process is bounded by $C/N^{1/2}$, and C is some constant. The connection can be used to solve the SLE driven by the OU process in a clumsy way.

We now discuss the difference of the various uses of the terms, Markovian and non-Markovian. For the Gaussian white noise process used in the HSR model, it is assumed that the Markov process as defined in eq 25 has $\langle x(t_0)x(t_1)\rangle = \Delta\delta(t_1 - t_0)$. The delta function approximation is often referred to as the "Markovian approximation" for the second-order master equation. However, it is different from the Markov property of the random process. Contrary to the definition of "Markovian" in the HSR model, a SLE driven by the dichotomic/Gauss−Markov process is a non-Markovian model with an exponential memory kernel, although it is a Markov process. Only in the limit of infinitely short exponential memory do the two uses of the term, Markovian, coincide. As for the non-Markovian process, it is a different concept. Briefly, when a process is non-Markovian, the covariance matrix M is a full matrix instead of tridiagonal for the Gaussian process. In summary, a SLE driven by a non-Markovian process and a non-Markovian second-order master equation are different concepts, which are not equivalent.[69]

AUTHOR INFORMATION

Corresponding Author
*E-mail: silbey@mit.edu.

ACKNOWLEDGMENT

This material is based upon work supported as part of the Center for Excitonics, an Energy Frontier Research Center funded by the U.S. Department of Energy, Office of Science, Office of Basic Energy Sciences under Award No. DE-SC0001088.

REFERENCES

(1) Engel, G. S.; Calhoun, T. R.; Read, E. L.; Ahn, T.; Mancal, T.; Cheng, Y. C.; Blankenship, R. E.; Fleming, G. R. *Nature* **2007**, *446*, 782–786.
(2) Collini, E.; Wong, C. Y.; Wilk, K. E.; Curmi, P. M. G.; Brumer, P.; Scholes, G. D. *Nature* **2010**, *463*, 644–647.
(3) Chen, X.; Silbey, R. J. *J. Chem. Phys.* **2010**, *132*, 204503.
(4) Mukamel, S.; Oppenheim, I.; Ross, J. *Phys. Rev. A* **1978**, *17*, 1988–1998.
(5) Yoon, B.; Deutch, J. M.; Freed, J. H. *J. Chem. Phys.* **1975**, *62*, 4687–4696.
(6) Haken, H.; Strobl, G. *Z. Phys. A* **1973**, *262*, 135–148.
(7) Haken, H.; Reineker, P. *Z. Phys. A* **1972**, *249*, 253–268.
(8) Jackson, B.; Silbey, R. J. *J. Chem. Phys.* **1981**, *75*, 3293–3296.
(9) Rips, I. *Phys. Rev. E* **1993**, *47*, 67–79.
(10) Kenkre, V. M. *Phys. Rev. B* **1975**, *11*, 1741–1745.
(11) Sumi, H. *J. Chem. Phys.* **1977**, *67*, 2943–2954.
(12) Reineker, P.; Kassner, K. *J. Lumin.* **1988**, *40−41*, 467–468.
(13) Reineker, P.; Kaiser, B.; Kraus, V.; Jayannavar, A. M.; Warns, C. *J. Lumin.* **1992**, *53*, 125–128.

(14) Kraus, V.; Reineker, P. *Phys. Rev. A* **1991**, *43*, 4182–4191.
(15) Kotelenez, P. *Stochastic Ordinary and Stochastic Partial Differential Equations: Transition from Microscopic to Macroscopic Equations*, 1st ed.; Springer: New York, 2007.
(16) van Kampen, N. G. *Stochastic Processes in Physics and Chemistry*, 3rd ed.; North Holland: Amsterdam, the Netherlands, 2007.
(17) Bourret, R. C. *Can. J. Phys.* **1965**, *43*, 619–639.
(18) Tanimura, Y. *J. Phys. Soc. Jpn.* **2006**, *75*, 82001.
(19) Shapiro, V. E.; Loginov, V. M. *Physica A* **1978**, *91*, 563–574.
(20) Ankerhold, J.; Pechukas, P. *EPL* **2000**, *52*, 264.
(21) Kraus, V.; Reineker, P. *Phys. Rev. A* **1991**, *43*, 4182–4191.
(22) Warns, C.; Barvik, I.; Reineker, P.; Neidlinger, T. *Chem. Phys.* **1995**, *194*, 117–131.
(23) Bourret, R. C.; Frisch, U.; Pouquet, A. *Physica* **1973**, *65*, 303–320.
(24) Ehsanur, R. Q.; Karasulu, M. *Ann. Nucl. Energy* **1979**, *6*, 133–143.
(25) Tanimura, Y.; Kubo, R. *J. Phys. Soc. Jpn.* **1989**, *58*, 101.
(26) Loginov, V. M. *Acta Phys. Pol., B* **1996**, *27*, 693–735.
(27) Fox, R. F. *Phys. Rev. A* **1991**, *43*, 2649–2654.
(28) Warns, C.; Reineker, P. *Springer Proc. Phys.* **1992**, *69*, 209.
(29) Warns, C.; Barviki, I.; Reineker, P. *Phys. Rev. E* **1998**, *57*, 3928.
(30) Warns, C. Ph.D. Thesis, University of Ulm, 1992.
(31) Barvik, I.; Warns, C.; Neidlinger, T.; Reineker, P. *Chem. Phys.* **1999**, *173*, 240.
(32) Kaiser, B. Ph.D. Thesis, University of Ulm, 1988.
(33) Kraus, V. Ph.D. Thesis, University of Ulm, 1989.
(34) Wubs, M.; Knoester, J. *Chem. Phys. Lett.* **1998**, *284*, 63–70.
(35) van Den Broeck, C. *J. Stat. Phys.* **1983**, *31*, 467–483.
(36) Fox, R. F. *J. Math. Phys.* **1972**, *13*, 1196–1207.
(37) Brissaud, A.; Frisch, U. *J. Math. Phys.* **1974**, *15*, 524–534.
(38) Scholes, G. D.; Fleming, G. R. *Adventures in Chemical Physics*; John Wiley & Sons, Inc.: Hoboken, New Jersey, 2005; pp 57−129.
(39) Cheng, Y. C.; Silbey, R. J. *Phys. Rev. Lett.* **2006**, *96*, 028103.
(40) Ishizaki, A.; Fleming, G. R. *Proc. Natl. Acad. Sci. U.S.A.* **2009**, *106*, 17255–17260.
(41) Nibbering, E. T. J.; Wiersma, D. A.; Duppen, K. *Phys. Rev. Lett.* **1991**, *66*, 2464–2467.
(42) Yang, M.; Fleming, G. R. *Chem. Phys.* **2002**, *275*, 355–372.
(43) Weber, J. *Phys. Rev.* **1956**, *101*, 1620–1626.
(44) Pottier, N.; Mauger, A. *Physica A* **2001**, *291*, 327–344.
(45) Toda, M.; Kubo, R.; Saito, N.; Hashitsume, N. *Statistical Physics: Nonequilibrium statistical mechanics*, 2nd ed.; Springer: 1991.
(46) Hida, T.; Hitsuda, M. *Gaussian Processes*; American Mathematical Society: 2007.
(47) Thorwart, M.; Eckel, J.; Reina, J.; Nalbach, P.; Weiss, S. *Chem. Phys. Lett.* **2009**, *478*, 234–237.
(48) Makarov, D. E.; Makri, N. *Chem. Phys. Lett.* **1994**, *221*, 482–491.
(49) Prior, J.; Chin, A. W.; Huelga, S. F.; Plenio, M. B. *Phys. Rev. Lett.* **2010**, *105*, 050404.
(50) Stockburger, J. T.; Mak, C. H. *Phys. Rev. Lett.* **1998**, *80*, 2657–2660.
(51) Abramavicius, A.; Palmieri, B.; Voronine., D. V.; Sanda, F.; Mukamel, S. *Chem. Rev.* **2009**, *109*, 2350–2408.
(52) Ishizaki, A.; Tanimura, Y. *J. Phys. Soc. Jpn.* **2005**, *74*, 3131–3134.
(53) van Grondelle, R.; Novoderezhkin, V. I. *Phys. Chem. Chem. Phys.* **2006**, *8*, 793–807.
(54) Cheng, Y. C.; Fleming, G. R. *Annu. Rev. Phys. Chem.* **2009**, *60*, 241–262.
(55) Amerongen, H. V.; Valkunas, L.; Grondelle, R. V. *Photosynthetic Excitons*; World Scientific Publishing Company: 2000.
(56) Panitchayangkoon, G.; Hayes, D.; Fransted, K.; Caram, J.; Harel, E.; Wen, J.; Blankenship, R.; Engel, G. *Proc. Natl. Acad. Sci. U.S.A.* **2010**, *107*, 12766–12770.
(57) Plenio, M. B.; Huelga, S. F. *New J. Phys.* **2008**, *10*, 113019.
(58) Caruso, F.; Chin, A. W.; Datta, A.; Huelga, S. F.; Plenio, M. B. *Phys. Rev. A* **2010**, *81*, 062346.
(59) Mohseni, M.; Rebentrost, P.; Lloyd, S.; Aspuru-Guzik, A. *J. Chem. Phys.* **2008**, *129*, 174106.
(60) Rebentrost, P.; Mohseni, M.; Kassal, I.; Lloyd, S.; Aspuru-Guzik, A. *New J. Phys.* **2009**, *11*, 33003.
(61) Redfield, A. G. *IBM J. Res. Dev.* **1957**, *1*, 19–31.
(62) Lindblad, G. *Commun. Math. Phys.* **1976**, *48*, 119–130.
(63) Liu, F.; Wu, J.; Shen, Y.; Cao, J.; Silbey, R. J. *New J. Phys.* **2010**, *12*, 105012.
(64) Cao, J.; Silbey, R. J. *J. Phys. Chem. A* **2009**, *113*, 13825–13838.
(65) Hoyer, S.; Sarovar, M.; Whaley, K. B. *New J. Phys.* **2010**, *12*, 65041.
(66) Lisette, D. B.; Coca, M.; Knoester, J. *J. Chem. Phys.* **1999**, *110*, 2208–2218.
(67) Fox, R. F.; Uhlenbeck, G. E. *Phys. Fluids* **1970**, *13*, 1893.
(68) Fox, R. F. *Phys. Rep.* **1978**, *48*, 179–283.
(69) van Kampen, N. *Braz. J. Phys.* **1998**, *28*, 90–96.